

Estimation of Radioactive Heat Production from Airborne Spectral Gamma-ray Data of Gebel Duwi Area, Egypt

Salem, Ahmed

Airborne Geophysics Department, Nuclear Materials Authority of Egypt:Currently Postdoctoral,
Department of Earth Resources Engineering

Elsirafy, Abouelhoda

Airborne Geophysics Department, Nuclear Materials Authority of Egypt:Currently Postdoctoral,
Department of Earth Resources Engineering

Aref, Alaa

Airborne Geophysics Department, Nuclear Materials Authority of Egypt:Currently Postdoctoral,
Department of Earth Resources Engineering

Ismail, Atef

Airborne Geophysics Department, Nuclear Materials Authority of Egypt:Currently Postdoctoral,
Department of Earth Resources Engineering

他

<https://hdl.handle.net/2324/3325>

出版情報：九州大学工学紀要. 64 (2), pp.135-146, 2004-06. 九州大学大学院工学研究院
バージョン：
権利関係：



Estimation of Radioactive Heat Production from Airborne Spectral Gamma-ray Data of Gebel Duwi Area, Egypt

by

Ahmed SALEM^{1*}, Abouelhoda ELSIRAFY¹, Alaa AREF¹, Atef ISMAIL¹, Sachio EHARA²
and Keisuke USHIJIMA²

(Received March 22, 2004)

Abstract

A map of radioactive heat production was constructed from airborne spectral gamma-ray data of Gebel Duwi area, Egypt. The study area possesses a range of radioactive heat production varying from 0.21 μWm^{-3} to 3.09 μWm^{-3} . Sedimentary rocks in the Gebel Duwi area have higher heat production values (0.25 μWm^{-3} to 3.09 μWm^{-3}) than the crustal average for sedimentary rocks. The average heat production of granitic rocks is below the crustal average value (1.48 μWm^{-3}) for the granites. The high values of heat production in the sedimentary rocks are mainly related to the relative increase of uranium content in the Duwi phosphate formation. The reduced heat production of the granitic rocks indicates that additional mantle components combine with the crustal radioactive heat production to the heat sources in the Gebel Duwi area.

Keywords: Airborne, Radioactive heat production, Gebel Duwi, Egypt, Red Sea, Gamma-ray spectrometry

1. Introduction

The Red Sea is clearly a region of high heat flow. More than 90 per cent of the heat flow measurements exceed the world mean and high values extend to the coasts where they are nearly twice the world mean¹²⁾. Accordingly, the countries bordering the Red Sea have good prospects for the utilization of geothermal resources on their Red Sea margins¹⁶⁾.

The Gebel Duwi area lies on the western side of the Red Sea margin in Egypt (**Fig. 1**). In the Gebel Duwi area, geothermal gradients were measured at only 3 shallow borehole sites. The gradients were measured at Duwi and Abu Shegala (12 °C/km and 50 °C/km, respectively) in sedimentary rocks and at Hamrawein (29 °C/km) in Precambrian basement outcrops¹⁶⁾. Characterization of the geothermal setting of the Gebel Duwi area based on only

¹ Airborne Geophysics Department, Nuclear Materials Authority of Egypt

* Currently Postdoctoral, Department of Earth Resources Engineering

² Professor, Department of Earth Resources Engineering

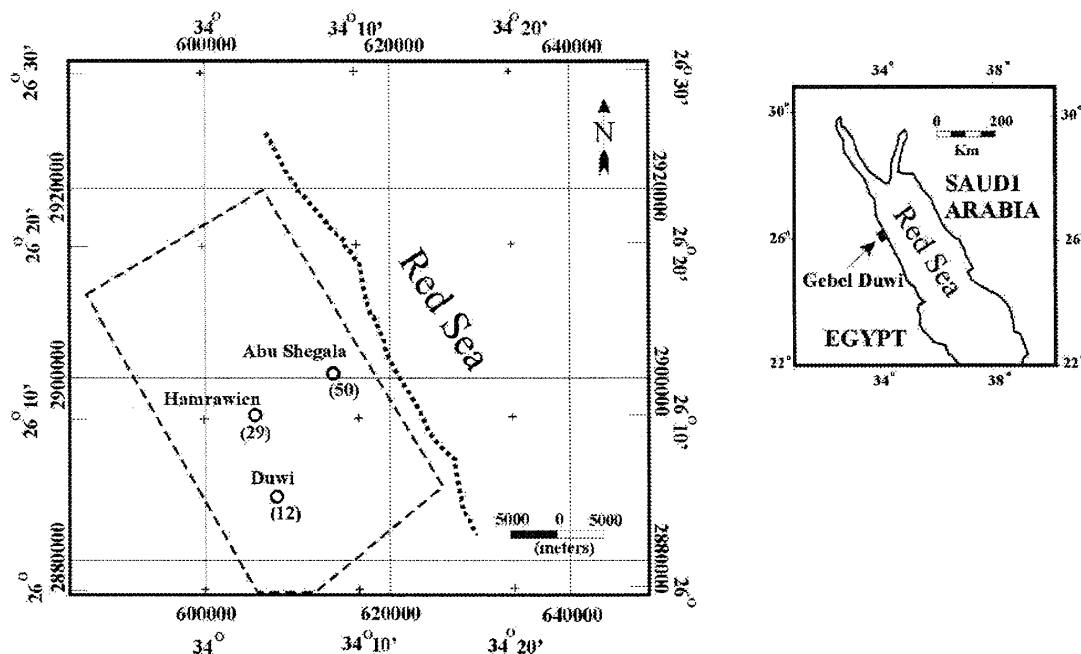


Fig. 1 The location of the Gebel Duwi area and layout of the airborne survey (dashed box). Values beside circles indicate the measured geothermal gradients ($^{\circ}\text{C}/\text{km}$) in shallow bore hole sites¹⁸⁾.

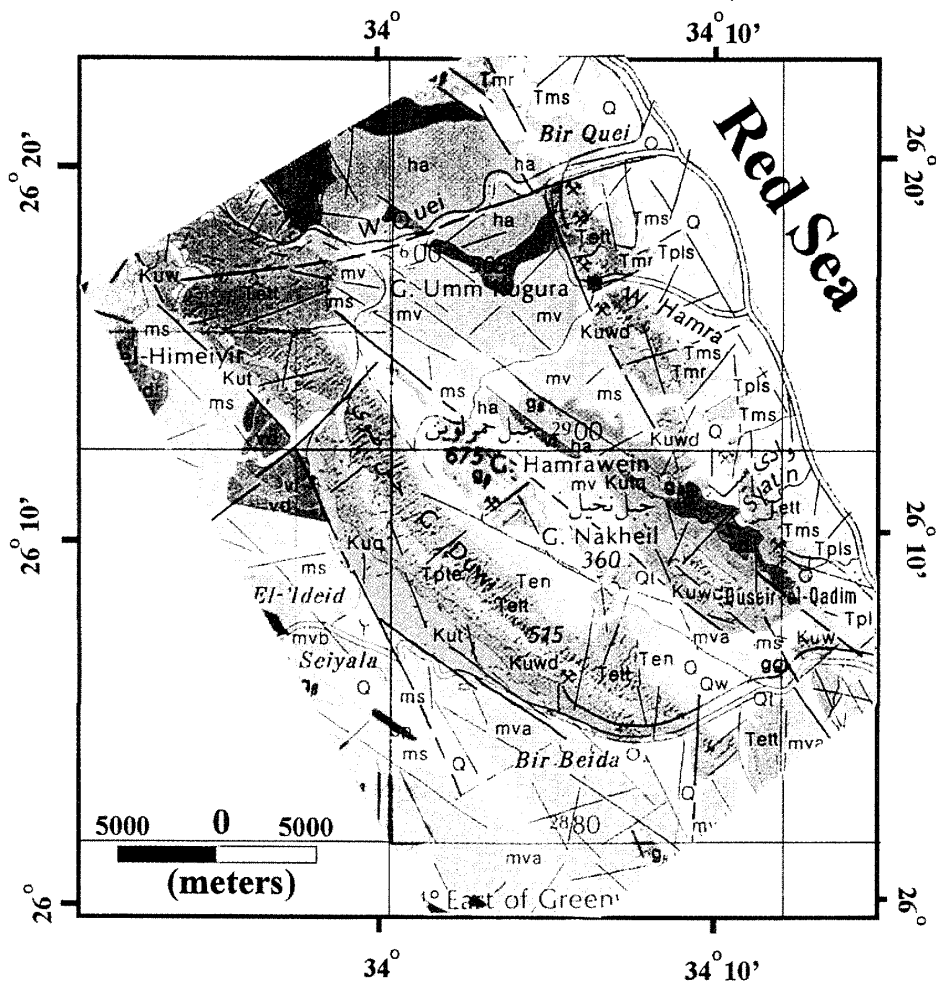
three, very shallow ($<300\text{m}$) geothermal gradient observations is unacceptable. A more comprehensive study is required to characterize the geothermal setting and identify possible prospects for further geothermal exploration.

Although direct measurements of thermal gradients in deep boreholes provide accurate data, it requires expensive drilling. Geophysical surveys provide a relatively inexpensive but less accurate data. The Gebel Duwi area (**Fig. 1**), as a part of the Egyptian Eastern Desert, was surveyed during a systematic aerial gamma-ray and magnetic survey conducted by Aero Service Division, Western Geophysical Company of America in 1983. The survey was designed to provide data, which would be of assistance in identifying and assessing the mineral, petroleum and ground water resources of the region³⁾.

The main purpose of this paper is to provide new insights on the geothermal setting of the Gebel Duwi area based on the existing airborne spectral gamma-ray data. We attempt to map surface radioactive heat production from the airborne gamma-ray data. Radioactive heat production can be used for several purposes⁵⁾. It can be used for explanation of temperature variations with depth and interpretation of existing heat flow variations. Also it can be used in selecting suitable new sites for making heat flow and/or heat production measurements.

2. Geological setting of the Gebel Duwi area

The Gebel Duwi area (**Fig. 2**) can be divided into two parts; the Duwi range and the coastal plain. The Duwi range consists of a long sharp ridge, elongated in the northwest direction that drops precipitously to the southwest and slopes gently to the northeast. The elevation of this ridge ranges between 450 and 545 m above sea level (ASL). The coastal plain is generally smooth in outline, with no sharp bends or bays. It slopes gently seaward. The relief of the coastal plain is generally low and varies from 6 to 30 m ASL.



Legend

Qw	Wadi deposits	Tpe	Esna Fm.		Dokhan volcanic
Q	Quaternary deposits	Tpte	Tarawan Fm.		Alkaline granite
Tpls	Pliocene deposits	Kud	Dakhla Fm.		Hammamat clastics
Tpls	Shagra Fm.	Kuw	Duwi Fm.		Metasediments
Tms	Um Gheig Fm.	Kutq	Quseir Fm.		Acidic metavolcanic
Ten	Nakheil Fm.				Metavolcanic
Tett	Thebes Fm.				

Fig. 2 Geological map of the Gebel Duwi area⁷⁾.

Geologically, the Gebel Duwi area is a part of the Central Eastern Desert of Egypt. Division of the Eastern Desert of Egypt into northern, central and southern sections is based on basement type²⁶⁾. The Central Eastern Desert was formed by collapse of a small ocean basin or back arc basin²²⁾. Several authors have investigated the stratigraphy of the Central Eastern Desert of Egypt^{4),2)}. In general, the sedimentary rocks of the Gebel Duwi area are separable into two great divisions: the pre-rifting Cretaceous-Eocene group and the post-rifting Oligocene and later sediments group. The latter division exhibits a continuous succession from middle Miocene onward. The Cretaceous and Eocene deposits occupy the troughs of synformal-like folds within the crystalline hill ranges. The best example of the pre-rift series outcrops in the Gebel Duwi basin, where more than 1500 m of Cretaceous and Eocene stratigraphy is exposed from the bottom to the top. The marine upper Eocene and

Oligocene deposits are absent, indicating that the region must have undergone elevation changes during these two epochs²⁰).

Several authors have discussed the basement stratigraphy of the Central Eastern Desert of Egypt⁸). In general, the Central Eastern Desert is dominated by rocks of oceanic affinity such as mafic metavolcanic, gabbros, ultramafic and associated metasedimentary rocks⁶). The oldest rock units comprise a mafic-ultramafic sequence having ophiolite characteristics. In this region, the metavolcanic rocks represent pillow tholeiite basalts, which developed on gabbroic and ultramafic substrata of this oceanic sequence²⁵). Conformably overlying these oceanic substrata are thick sequences of subduction related immature volcanogenic metasediments, which are conformably overlain by, and interfinger with, island arc type of calc-alkaline volcanic rocks. A major regional unconformity separates the ophiolitic, metasediments, metavolcanic, granitic and Dokhan volcanic rocks from a generally unmetamorphosed, dominantly terrigenous sequence of molasse type sediments known as Hammamat group⁹). These Hammamat sediments were deposited in intracratonic basins and were preserved in down-faulted blocks, or in topographic lows.

3. Airborne spectral gamma-ray data

The airborne spectral gamma-ray survey was conducted along a set of parallel flight lines oriented in a northeast-southwest direction, perpendicular to the prevailing geologic strike, at one km spacing³). Spectral radiometric measurements were recorded with 93 m (300 feet) sampling interval at a nominal sensor altitude of 120 m (terrain clearance). The survey was conducted using twin-engine Cessna-404 Titan aircraft. This type of airplane can be operated within a speed range between 222 km/h to 315 km/h. A high sensitivity 256-channel airborne gamma-ray spectrometer with a primary 50.3 liters sodium iodide, thallium activated detector was used. For more details on the survey equipment used and flight operations, the reader is referred to the final operation report³). Discussion of airborne radiometric surveying techniques, including instrumentation, reporting methods, system calibration, and gamma-ray energy windows, is given by the International Atomic Energy Agency¹³).

Figures 3 to 5 show color maps of the apparent surface concentrations of radioelements [potassium (K) in %, equivalent uranium (eU) and thorium (eTh) in ppm, respectively]³). **Figure 6** displays a ternary image combining the three radio-elements. Generally, ternary plots of the radio-elements usually give a superior image of the geology. This can be seen in the well correlation between the ternary image (**Fig. 6**) and the mapped geology (**Fig. 2**). Separate radio-element maps are also useful to identify certain rock types. For example, the boundaries of the Duwi sedimentary basin can be delineated from the U map (**Fig. 4**). The K and Th maps (**Figs. 3 and 5**), on the other hand, illustrate the boundaries of igneous and metamorphic rocks. In the Gebel Duwi area, higher uranium values extend to more than 12 ppm and are observed over Duwi formation. This unit is composed of about 98 m of phosphatic limestone of Santonian to Campanian age²). Mansour and Farouk¹⁵) pointed out that the uranium content increases with increasing phosphate in the Duwi formation. Other significant radioactive anomalies are not observed.

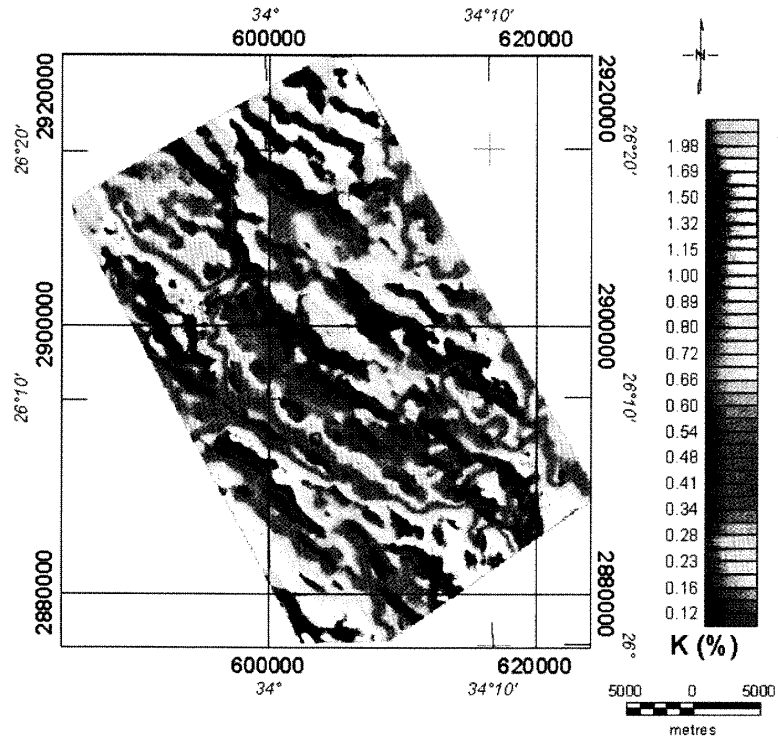


Fig. 3 Potassium color map of the Gebel Duwi area³⁾.

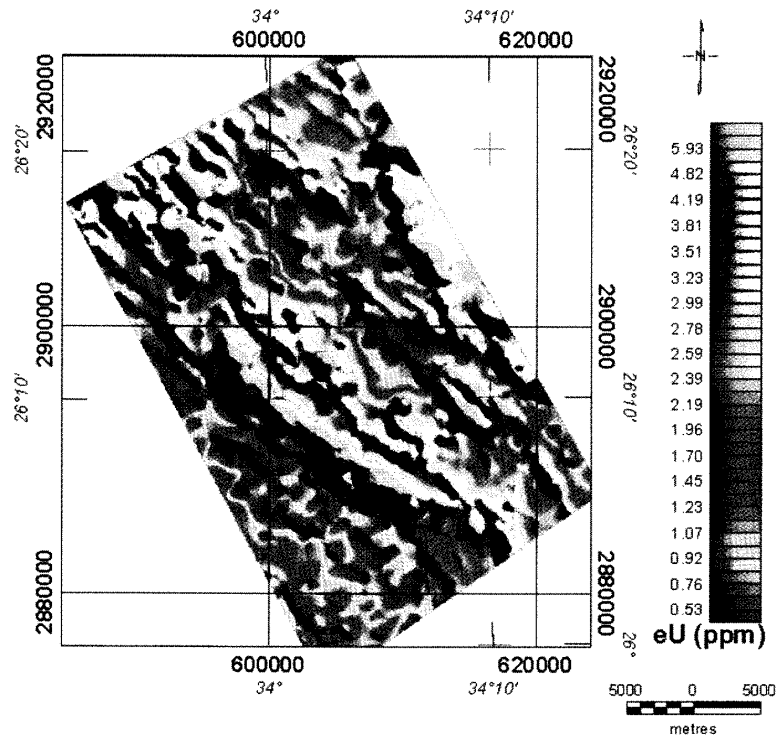


Fig. 4 Equivalent uranium color map of the Gebel Duwi area³⁾.

4. Mapping radioactive heat production

Rybach¹⁹⁾ published an empirical equation to calculate the radioactive heat production of a given rock sample using this expression

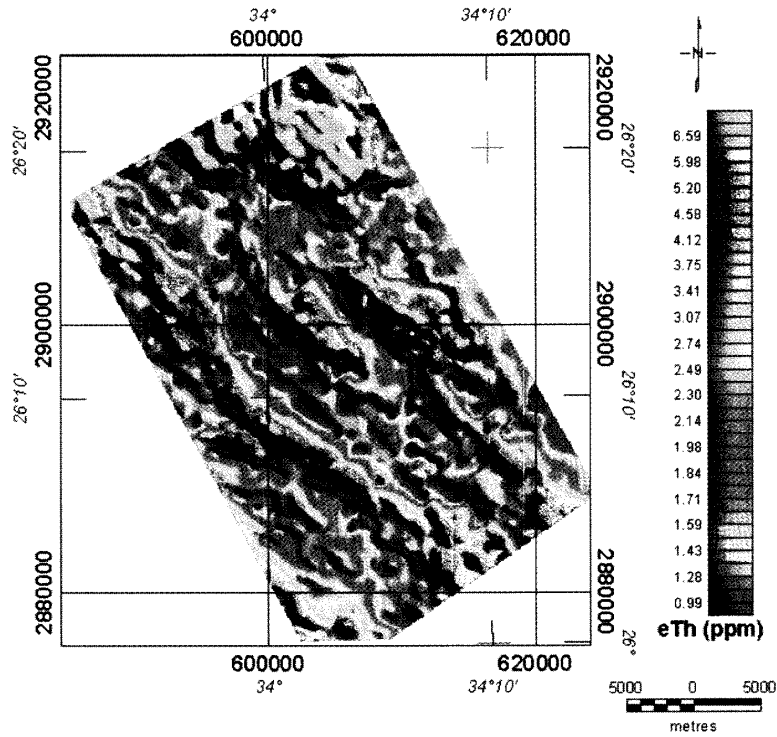


Fig. 5 Equivalent thorium color map of the Gebel Duwi area³⁾.

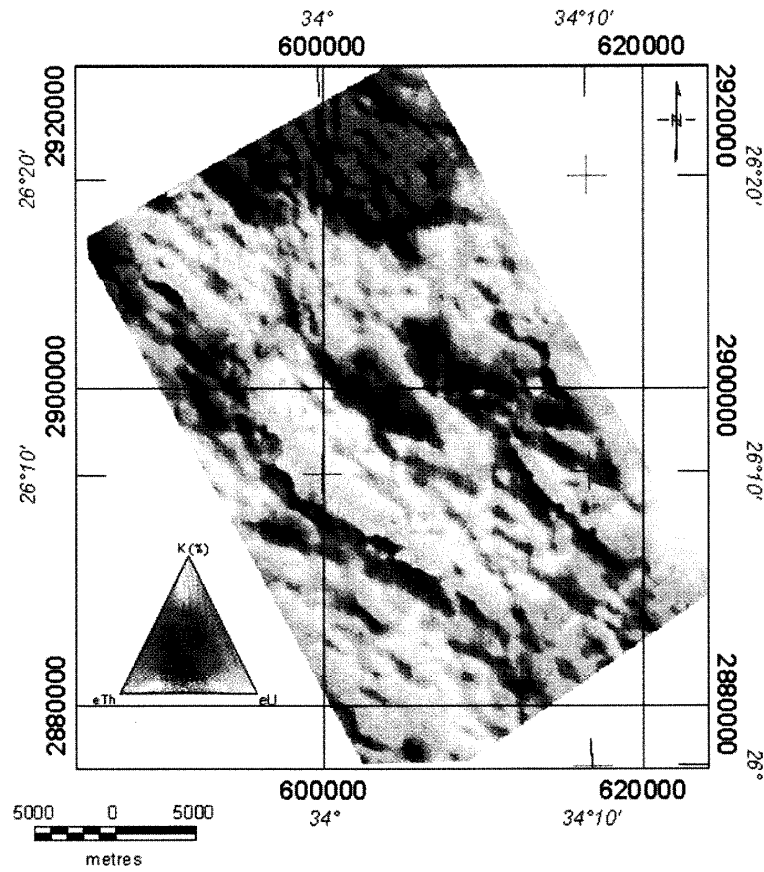


Fig. 6 Ternary image constructed from the radio-elements (K (%), eU, and eTh) maps.

$$A(\mu Wm^{-3}) = \rho(0.0952C_U + 0.0256C_{Th} + 0.0348C_K), \quad (1)$$

where ρ is the density of rock (g/cm^3) and C_U , C_{Th} and C_K are the concentrations of U and Th in ppm and K in %, respectively. In Rybach's formula, it is first necessary to know the density and the concentration of radio-elements U, Th and K in the rock. Radioactive heat production has been calculated from concentrations of radio-elements measured in the laboratory¹⁰⁾ and directly from gamma-ray logs⁵⁾. Also radioactive heat production has been estimated from airborne gamma-ray data^{18),27)}.

To calculate radioactive heat production from airborne gamma-ray data, both the type of rocks and their boundaries must be well identified beforehand. Also the average density for each rock unit should be known or can be assumed. The Gebel Duwi area consists of large separable units of igneous and metamorphic rocks as well as ranges of sedimentary rocks preserved within the crystalline hills. **Figure 2** shows that most sedimentary formations have narrow outcrops elongated in the northwest-southeast direction. Although the flight lines are perpendicular to the outcrop of the sedimentary formations, calculation of reliable radioactive heat production for each of the different sedimentary rocks is difficult due to their narrow exposure. For an airborne survey at a height of 120 m, speeds of 200 km/h to 300 km/h and data accumulation at one sample per second, few gamma-rays are recorded from each formation. Furthermore, the spectral gamma-rays recorded over a certain formation include the radiation effects of neighboring formations. For the sake of simplicity, the sedimentary rocks in the study area were grouped as representing one rock unit. Consequently, the following six rock units: sedimentary, metavolcanic, metasediments, granitic, Hammamat sediments and Dokhan volcanic rocks were assigned for further calculation of the radioactive heat production based on the concentrations of potassium, uranium and thorium within each rock unit. In this work, we calculated the average density for each rock unit (**Table 1**) from the densities published by Shabban²¹⁾. Generally, the density values obtained for basement samples ranged from 2.59 g/cm^3 for granites, to 2.92 g/cm^3 for more basic diorites and gabbros. Densities of sedimentary rocks ranged from 2.00 g/cm^3 for sandstone to 2.62 g/cm^3 for silicified limestone. The boundaries of the six rock units were outlined (**Fig. 7**) and the radio-element concentrations (K(%), eU and eTh) within each rock unit were isolated. Radioactive heat production values for each rock unit were calculated based on Eq. (1). Then the results are summarized in **Table 2** and illustrated as a map of the radioactive heat production in **Fig. 8**.

Table 1 Average density for each rock unit²¹⁾.

Rock	Density (g/cm^3)
Sedimentary	2.41
Metasediments	2.62
Metavolcanic	2.64
Hammamat	2.61
Dokhan volcanic	2.60
Granite	2.59

5. Discussion

The estimated radioactive heat production values (**Fig. 8**) are governed by the amount of uranium, thorium, and potassium measured from airborne survey and, therefore, they are surface or apparent values. In general, the radioactive heat production varies greatly with rock type. This can be explained by the good correlation between the radioactive heat production map (**Fig. 8**) and the mapped geology (**Fig. 2**). The area possesses a range of radioactive heat production varying from 0.21 μWm^{-3} to 3.09 μWm^{-3} . The higher average values (**Table 2**) are obtained for Dokhan volcanic and granitic rocks (1.42 μWm^{-3} and 1.48 μWm^{-3} , respectively), whereas the lowest average value is obtained for metasedimentary

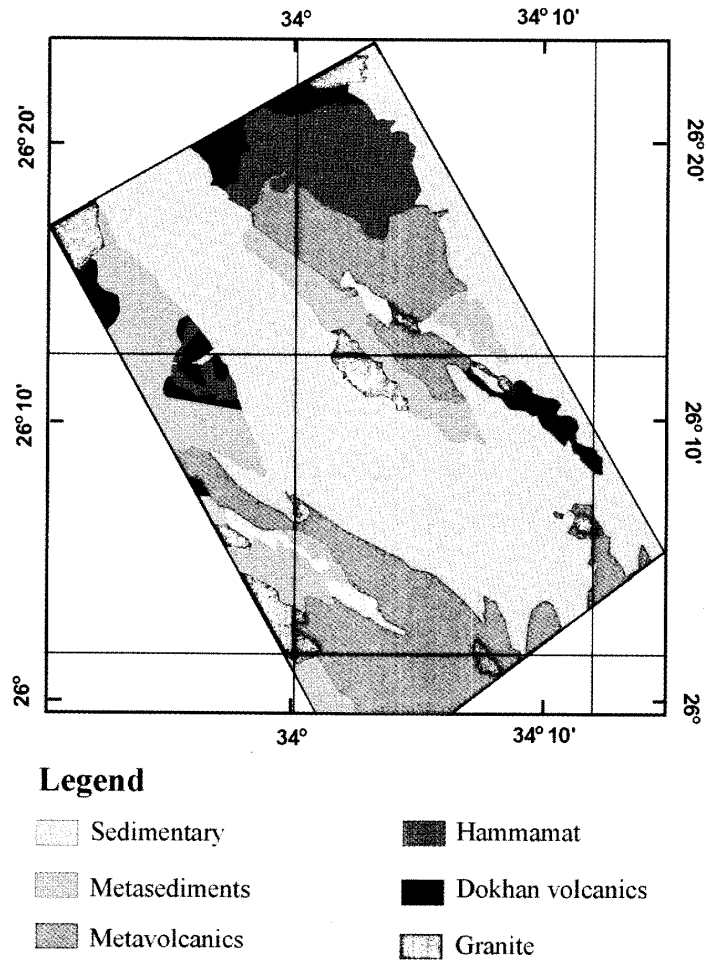


Fig. 7 Rock units map of the Gebel Duwi area. Average density for each rock unit (**Table 1**) and radio-elements (K(%), eU, and eTh) within each rock unit were used to calculate the radioactive heat production.

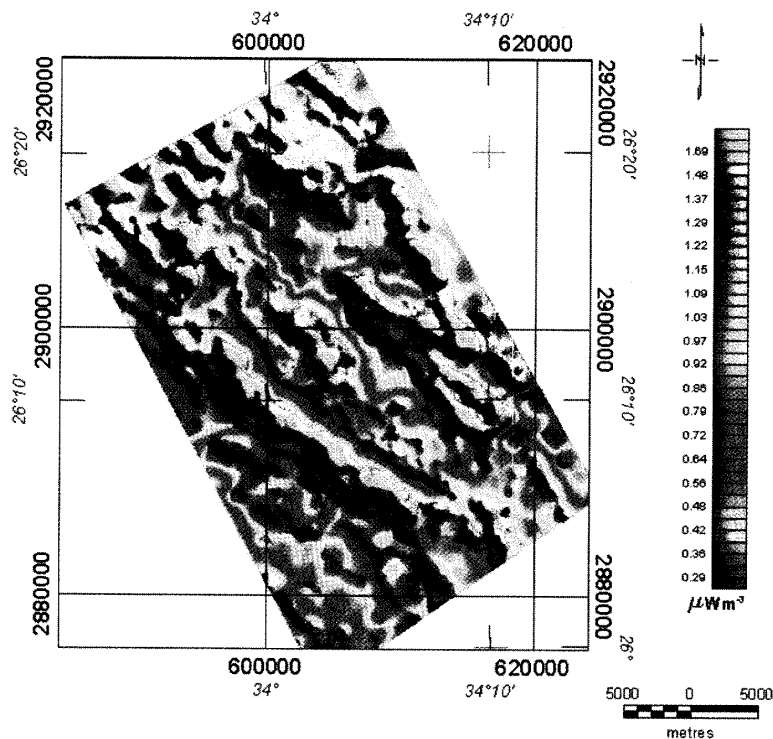


Fig. 8 Radioactive heat production color map of the Gebel Duwi area.

rocks ($0.43 \mu\text{Wm}^{-3}$). A clear similarity between the statistical characteristics of radioactive heat production (mean and standard deviation) corresponding to Dokhan volcanic and granitic rocks is seen (**Table 2**) and indicates a definitive similarity in the petrophysical properties. The radioactive heat production distribution for metasediments and metavolcanic is completely different. This may be attributed to the difference in the degree of metamorphism and deformation between metavolcanic and metasediments. However, radioactive heat production may exhibit some irregularity due to the dissimilarity in the geochemical behavior of U, Th, and K during the metamorphism process, which determines the distribution of the natural radio-elements.

Table 2 Radioactive heat production corresponding to each rock unit (in μWm^{-3}).

Rock unit	N*	Range		Mean	Std. Dev.
		Min	Max		
Sedimentary	665	0.25	3.09	1.19	0.42
Metasediments	889	0.21	1.42	0.43	0.13
Metavolcanic	1498	0.37	2.58	0.95	0.36
Hammamat	592	0.62	2.41	1.16	0.21
Dokhan volcanic	168	0.82	2.40	1.42	0.21
Granite	63	1.17	1.96	1.48	0.19

* N is number of data points within each rock unit

Comparative inspection of the computed averages of the apparent heat production estimated by this study (**Table 2**) and that for the crustal rocks published by Rybach¹⁹⁾ produced the following two important observations regarding the heat generation of rocks in the study area. Firstly, the sedimentary rocks including Hammamat sediments show values ($0.25 \mu\text{Wm}^{-3}$ to $3.09 \mu\text{Wm}^{-3}$) higher than those given for the crustal sedimentary rocks ($0.33 \mu\text{Wm}^{-3}$ to $1.8 \mu\text{Wm}^{-3}$). Secondly, the granitic rocks in the Gebel Duwi area show an average value ($1.48 \mu\text{Wm}^{-3}$) below the average for the crustal granites ($2.4 \mu\text{Wm}^{-3}$). The high values of heat production in the sedimentary rocks are mainly related to the relative increase of uranium content in Duwi phosphate formation. The elevated average value of Hammamat sediments is mainly attributed to the intrusion of the successive pulses of the younger igneous bodies. This is supported by field observations, which indicated that the topmost horizon of these sediments contains subangular to subrounded pebbles, as well as some granitic cobbles derived from older basement units¹⁾. The elevated heat production values of the sedimentary rocks may signify shallow heat flow resources. The reduced heat production for the granitic rocks appears to be related to a relative decrease in uranium content.

Although the estimated radioactive heat production values are realistic and lie in the range given for the crustal rock, laboratory or ground measurements are required to check the validity of the estimated heat production from airborne data. We have carried out some random ground spectral gamma-ray measurements over the granite of the Hamarawin site. A portable multichannel gamma-ray spectrometer model GS-256 was used. This instrument includes a detector assembly of 0.34 liters of crystal (21 cubic inches). The spectrometer was calibrated using the concrete calibration pads of the Nuclear Materials Authority of Egypt. The measured window count rates have been subjected to background and stripping correction. These reduced count rates were converted into concentration units recommended by the International Atomic Energy Agency¹³⁾. The sensitivity factors were $3.02 \text{ counts} \cdot \text{s}^{-1} \cdot (\% \text{ K})^{-1}$, $0.29 \text{ counts} \cdot \text{s}^{-1} \cdot (\text{ppm eU})^{-1}$, and $0.06 \text{ counts} \cdot \text{s}^{-1} \cdot (\text{ppm eTh})^{-1}$. The in-situ measurements of K, eU, and eTh were used with the average density of the granite of Hamarawin site to calculate the radioactive heat production (**Table 3**). The average

radioactive heat production calculated from ground gamma-ray measurements is $1.62 \mu \text{Wm}^{-3}$. The difference between this value and that estimated from airborne data ($1.48 \mu \text{Wm}^{-3}$) is relatively small. However, determination of representative heat production values from airborne data presents a problem. Radio-elements content can vary greatly within any intrusion depending on a variety of factors such as multiple phases, zonation and crystallization.

Table 3 Ground spectral gamma-ray data measured in the Granite of Hamrawien site.

Longitude	Latitude	K (%)	eU (ppm)	eTh (ppm)	Heat production (μWm^{-3})
34° 1.337'	26° 13.832'	3.3	5.1	3.3	1.77
34° 1.336'	26° 13.840'	5.0	4.9	3.6	1.89
34° 1.591'	26° 13.627'	4.6	3.4	5.7	1.63
34° 1.627'	26° 13.646'	3.8	5.7	2.3	1.90
34° 1.582'	26° 13.577'	4.2	5.6	6.2	2.17
34° 1.637'	26° 13.649'	3.9	1.5	0.9	0.78
34° 2.098'	26° 13.554'	4.7	2.7	3.6	1.32
34° 2.361'	26° 13.323'	5.6	4.4	4.0	1.85
34° 2.640'	26° 13.089'	4.5	2.0	2.3	1.05
34° 2.792'	26° 13.985'	4.5	5.0	2.9	1.83
34° 2.811'	26° 13.001'	4.1	5.7	4.3	2.06
34° 2.889'	26° 12.979'	3.6	3.2	2.1	1.25

To assist in understanding the origin of the heat sources in the Gebel Duwi area, we calculated the reduced heat flow (q_1) at the granite of Hamrawein site (A similar analysis was not possible at the other two sites because the thermal measurements were made in sedimentary rocks). We assumed that the radio-elements content within the granite of Hamrawein site is normally distributed and no lateral contribution from the heat production of the other rock units. The reduced heat flow density q_1 is given by

$$q_1 = q_0 - DA_0, \quad (2)$$

where q_0 is the heat flow density at Hamrawein site (72.5 mW/m^2) using the observed thermal gradient ($29 \text{ }^\circ\text{C/km}$)¹⁶⁾ and assuming a thermal conductivity K of $2.5 \text{ Wm}^{-1}\text{ }^\circ\text{C}^{-1}$ given by Stacey²³⁾ as the average for igneous rocks, A_0 is the surface heat production based on the airborne spectral gamma-ray data ($1.48 \mu\text{Wm}^{-3}$) and D characterizes the heat distribution in the upper crust (assumed to be 14 km thick based on the published expanding spread profiles^{11),24)}). The reduced heat flow density is relatively high (51.3 mW/m^2) and indicates that high mantle heat flow combine with the radioactive heat production from the crustal heat sources in the Gebel Duwi area. Although radioactive decay is probably the greatest overall source of heat in the Earth's crust by a substantial factor, there are other sources that may be important in specific places¹⁴⁾. Therefore, we may suggest that the most probable source of the heat flow in the Gebel Duwi area seems to be high heat flow from the mantle, associated with the extension of the Red Sea. This assumption correlates well with the finding of Morgan et al.¹⁷⁾.

6. Conclusions

In this study, we attempted to provide new insights on the geothermal setting of the Gebel Duwi area based on the existing airborne spectral gamma-ray data. We mapped the radioactive heat production from the airborne gamma-ray data. The surveyed area possesses

a range of radioactive heat production varying from $0.21 \mu\text{Wm}^{-3}$ to $3.09 \mu\text{Wm}^{-3}$. The average heat production of granitic rocks is significantly low and indicates that additional mantle components combine with the radioactive heat production from the crustal heat sources in the Gebel Duwi area. Higher-resolution airborne survey data are highly recommended to assist in understanding the spatial distribution of K, U, and Th within each rock unit.

Acknowledgments

We greatly appreciate constructive and thoughtful comments of Dr. Robert Shives, and Dr. Sally Barritt. We would like to thank Jeffrey Gamey and Dr. Eslam Elawadi for suggesting a number of improvements in this manuscript. We would like to extend our thanks to Prof. L. Rybach for his help in discussing the use of aerial gamma-ray data in estimating the radioactive heat production. We are indebted to all members of the Airborne Geophysics Department of Nuclear Materials Authority of Egypt for their contribution to this study. Sincere thanks to all the staff of the Exploration Geophysical Laboratory of Kyushu University for their contribution and support during this work. The work of the first author on this paper is funded by the Japan Society for Promotion of Science (JSPS).

References

- 1) Abuzeid, H.T. 1988. The youngest Precambrian volcanic succession of Wadi Hamrawein, Eastern Desert, Egypt. Ph.D. thesis. Earth Sc. and Res. Inst. South Carolina, Columbia, USA.
- 2) Abdel Razzik T.M. 1972. Comparative studies on the upper Cretaceous-Early Paleocene sediments on the Red Sea coast, Nile Valley and Western Desert Egypt: 8th Arab Petroleum Congress, Algiers, May-June 1972, paper No. 71(B-3), 1-23.
- 3) Aero Service 1984. Final report on airborne magnetic/radiation survey in Eastern Desert, Egypt. Work completed for the Egyptian General Petroleum Corporation (EGPC). Six volumes: Aero Service, Houston, Texas, USA.
- 4) Akkad S. and Dardir A. 1966. Geology of Red Sea coast between Ras Shagara and Marsa Alam with short note on exploratory work at Gebel el Rusas Lead-Zink deposits Geological Survey of Egypt. paper No 35.
- 5) Bucker C. and Rybach L. 1996. A simple method to determine heat production from gamma-ray logs. *Marine and Petroleum Geology* 13, 373-375.
- 6) Cochran J.R. and Martinez F., 1988. Evidence from the northern Red Sea on the transition from continental to oceanic rifting. *Tectonophysics* 153, 25-53.
- 7) Conoco Inc., 1989, Stratigraphic lexicon and explanatory notes to the geological map of Egypt 1: 500,000. Conoco Inc., Cairo, Egypt, 1989, 26p.
- 8) Engel A.E.J., Dixon T.H. and Stern, R.J. 1980. Late Precambrian evolution of Afro-Arabian crust from ocean arc to craton: *Geological Society of America Bulletin* 91, 699-706.
- 9) El Ramly M.F. 1972. A new geological map for the basement rocks in the Eastern and Southwestern desert of Egypt: Scale 1:1,000,000. Annals of the Geological Survey of Egypt, 1-18.
- 10) Fernández M., Marzan I., Correia A., and Ramalho E., 1998. Heat flow, heat production, and lithosphere thermal regime in the Iberian Peninsula. *Tectonophysics* 291, 29-53.
- 11) Gaulier J.M., Pichon X. L.E, Lyberis N., Avedik F., Geli I., Moretti I., Deschamps A. and

- Hafez S., 1988. Seismic study of the crust of the northern Red Sea and Gulf of Suez: *Tectonophysics* 153, 55-88.
- 12) Girdler R.W. and Evans T.R., 1977. Red Sea heat flow. *Geophys. J. the Roy. Astr. Soc.* 51, 245-251.
 - 13) International Atomic Energy Agency 1991. Airborne gamma-ray spectrometer surveying: Tech. Rep. No.323. International Atomic Energy Agency.
 - 14) Jessop A.M., 1990. Thermal geophysics: Elsevier, Amsterdam.
 - 15) Mansour S.E. and Farouk A.F., 1998. Geology and radioactivity of the Red Sea phosphate deposits, 4th Conf. Nuc.Sc. & Appl. 1, 208-215.
 - 16) Morgan P., Boulos F.K., and Swanberg G.A. 1983. Regional geothermal Exploration in Egypt. *Geophysical prospecting* 31, 361-376.
 - 17) Morgan P., Boulos F.K., Hennin S.F., El-Serif A.A., El-Said A.A., Basta N.Z. and Melek, Y.S., 1985. Heat flow in eastern Egypt: the thermal signature of a continental breakup. *Geodynamics* 4, 107-131.
 - 18) Richardson, K.A., and Killeen, P.G., 1980. Regional radiogenic heat production mapping by airborne gamma-ray spectrometry; in Current Research, Part B, Geological Survey of Canada, Paper 80-1B, p.227-232.
 - 19) Rybach L. 1976. Radioactive heat production in rocks and its relation to other petrophysical parameters. *Pure & Appl. Geophysics* 114, 309-318.
 - 20) Said R. 1992. The geology of Egypt: Elsevier Science Ltd. Rotterdam, Netherlands.
 - 21) Shaaban M.A., 1973. Geophysical studies on the lead Zinc mining district between Quseir and Mersa Alam, Red Sea coast, Eastern Desert, Egypt: Ph.D. thesis No 568, Cairo University, Cairo, Egypt.
 - 22) Shackleton R.M., Ries A.C., Grahm R.H. and Fitches W.R., 1980. Late Precambrian ophiolite melange in the Eastern Desert of Egypt. *Nature* 285, 472-474.
 - 23) Stacey F. D., 1977. Physics of the Earth: New York, John Wiley and Sons, 2nd ed., 414pp.
 - 24) Steckler M.S. and Hobart M.A., 1986. Conrad Deep: a new northern Red Sea deep. Origin and implications for continental rifting. *Earth Planet. Sci. Lett.* 78, 18-32.
 - 25) Stern R.J., 1979. Late Precambrian ensimatic volcanism in the Central Eastern Desert of Egypt: Ph.D. thesis, San Diego, University of California, 210p.
 - 26) Stern R.J. and Hedge C.E., 1985. Geochronologic and isotopic constrains on Late Precambrian crustal evaluation in the Eastern Desert of Egypt: *Am. J. Sci.* 285, 97-127.
 - 27) Thompson, P.H., Judge, A.S., Charbonneau, B.W., Carson, J.M. and Thomas, M.D., 1996. Thermal regimes and diamond stability in the Archean Slave Province, Northwestern Canadian Shield, District of Mackenzie, Northwest Territories; in Current Research, 96-1E, Geological Survey of Canada, P. 135-146.